20

Digital Holography and Phase Retrieval

Hamootal Duadi[1], Ofer Margalit[1], Vicente Mico[2],
José A. Rodrigo[3], Tatiana Alieva[4], Javier Garcia[2] and Zeev Zalevsky[1]
[1]School of Engineering, Bar-Ilan University, Ramat-Gan 52900, [2]Departamento de Óptica, Universitat de València, c/Dr. Moliner, 50, 46100 Burjassot, [3]Instituto de Óptica (CSIC), Imaging and Vision Department. Serrano 121, Madrid 28006, [4]Universidad Complutense de Madrid, Facultad de Ciencias Fisicas, Ciudad Universitaria s/n, Madrid 28040,
[1]Israel
[2,3,4]Spain

1. Introduction

In imaging systems, digital as well as analogue, only the intensity is captured while the phase, containing the depth information and/or refractive index changes, is lost. Phase retrieval is the art of acquiring this information which is crucial in surface reconstruction, microscopy, location detection and depth measurements.
In this chapter we will first introduce holographic based methods, or the digital holography approach, as a solution to the phase retrieval problem. These methods use an optical setup, called an interferometer, which records the interference pattern between a reference beam and the analyzed wavefront. The interferometer image depends on the phase difference between the two beams; hence it holds the phase information. We will present a work of ours combining an interferometer setup with partial coherence and with specimen rotation. Note that instead of inspecting the contrast of the interference fringes one may use the contrast of the projected/reflected speckle patterns (self interference patterns) to map the axial domain.
We will then present phase retrieval methods based on wavefront propagation. This involves solving mathematical equations, related to physical conditions on the wavefront. Several numerical computational methods used for this task will be considered.
Further, we will overview the iterative approaches to the phase retrieval problem, discussing their abilities and limitations.
It will be shown that the iterative method based on multiple measurements allows more accurate and less noisy phase reconstruction. As an example we demonstrate the results of phase retrieval from the multiple images acquired in the gyrator domain.
Finally, some conclusions will be made.

2. Digital holography

One common method for acquiring the phase of an object is by digital holography. In regular holography, the interferometer image is written on film. Then the phase information

is reconstructed by illuminating the recording film with the correct reference beam. In digital holography the interferometer image is typically captured by a CCD camera and the reconstruction step is done using digital processing techniques. Holography based setups, named interferometer setups, are used to record the interference between a reference beam and the desired wavefront (Gabor, 1948; Leith & Upatnieks, 1962; Leith & Upatnieks, 1963; Leith & Upatnieks, 1964). This interference pattern contains the phase information, which can later be reconstructed. For the purpose of phase retrieval digital holography is used, since the idea is to use a CCD camera and digitally compute the missing phase information. Usage of in-line setups, i.e. phase shifting interferometer (Yamaguchi & Zhang, 1997; Bruning et. al., 1974; Xu et. al., 2002), permits the measurement of both phase and amplitude of an object. This is possible since the setup is an on axis setup, meaning that all beams are aligned to the optical axis (Fig. 1). The phase is recovered from the change in the diffraction pattern.

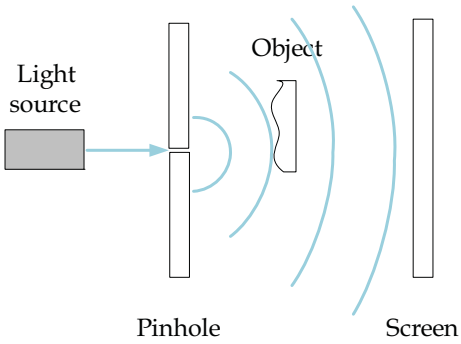

Fig. 1. Optical setup for in-line holography. A coherent wave propagates through a pinhole to create a point source. Partially scatters off an object, creating a highly magnified hologram on a screen.

The problem with holography is the phase wrapping ambiguity, i.e. the mapping range should not exceed one wavelength. Some methods are based upon the coherency of the light source (Rosen & Yariv, 1996), since interference fringes will only be generated within the coherence length. Various works propose tomographies with rotation of specimen or modification of illumination (Charriere et.al, 2006; Choi et. al, 2008). Other works propose using speckle properties as a unique axial characteristic (Karo, 1977; Cederquist et. al., 1988; Almoro et. al., 2009).

By combining an interferometer setup with partial coherence of a light source or specimen rotation (Zalevsky et. al., 2008), one may overcome the phase wrapping limitation. In the partial coherence method, a Michelson interferometer was used (Fig. 2). This interferometer splits the incoming beam to two optical paths. One path reaches a mirror and the other a reflective specimen. The two beams are combined together by a beam splitter (BS) to create an interferometer image relative to the surface profile of the specimen.

First the source's interference fringe contrast was mapped to create a reference lookup table (Table 1). This table includes the axial location corresponding to different fringe contrast values. One may see that in the very near field (up to 4mm) the fringe contrast is periodic, and in the farther field there is a linear decrease in the contras (maintaining the same

periodicity). Then, the 3D information is extracted from a single image using the lookup table. In the experimental results shown in Fig. 3, the depth difference between the two wafers placed on the mirror is approximately in the order of 20-30μm (Fig. 3. (a)) and 10-15μm (Fig. 3. (b)). One may see that the fringe contrast indeed changes for different depth positions. The fringe contrast, marked by C in the figures, is an indicator of the depth location, since the farther the object is, the lower the contrast. This method is a real time method, with tunable axial accuracy and without triangulation angle dependency.

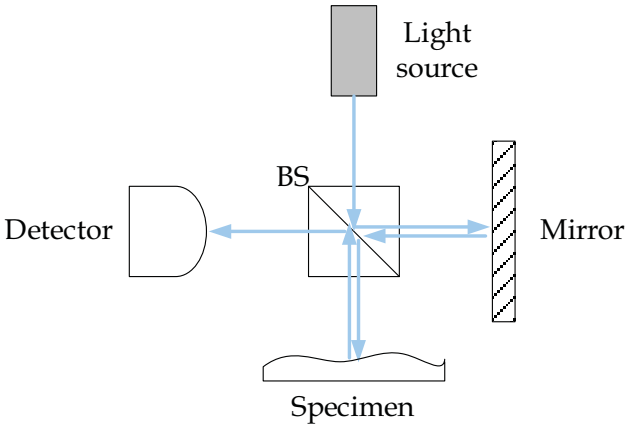

Fig. 2. Optical setup for Michelson interferometer. A coherent wave from the light source is spitted by the BS to two optical paths. One path leads to a mirror that reflects the ray back to the BS. The other path leads to a reflective specimen and back to the BS. The difference between the two optical paths depends on the profile of the specimen. Hence, by combining together the two rays, one receives an interferometer image relative to the profile of the specimen.

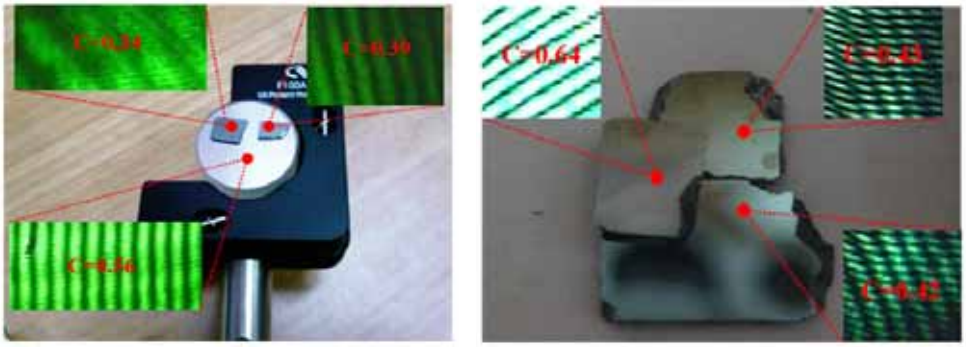

(a) (b)

Fig. 3. Image of the object used for the partial coherence experiment and the obtained interference pattern with the extracted local contrasts. (a) Two silicon wafers positioned on a mirror. (b). Two silicon wafers positioned on top of a third silicon wafer.

Path difference (mm)	Contrast
0	0.650
0.1	0.580
0.2	0.576
0.3	0.535
0.4	0.410
0.5	0.280
0.6	0.255
0.7	0.385
0.8	0.306
0.9	0.275
1.0	0.260
1.5	0.430
2.0	0.500
2.5	0.380
3.0	0.266
3.5	0.425
4.0	0.502
54.0	0.509
54.1	0.467
54.2	0.405
54.3	0.340
54.4	0.340
54.5	0.329
54.6	0.328
54.7	0.286
54.8	0.267
54.9	0.250
55.0	0.237

Table 1. Experimental lookup table of fringe contrast changes versus the difference betwean the two paths of the interferometer.

In the multiple angle setups, a Mach-Zehnder based interferometer was used, where the specimen was placed on a high precision rotation stage (Fig. 4). In this interferometer the input beam is split into two optical paths and the investigated sample is placed in one of these paths. The two beams are then combined by a BS to create an interferometer image relative to the depth profile of the sample.

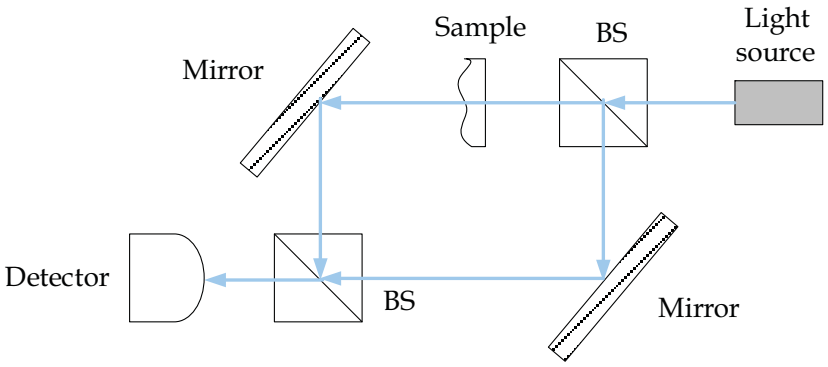

Fig. 4. Optical setup for Mach-Zender interferometer. A coherent wave from the light source is split by the BS to two optical paths. Both paths have the same optical distance and lead to a mirror that reflects the beam towards the second BS. However, a transparent sample is placed in one of the paths, which introduces a phase difference between the paths. The interferometer output of the BS is received by the detector.

In this setup, two images were captured while the angular orientation of the specimen was changed by the rotation stage and a 3D image was reconstructed using the following equations for the phase:

$$\left\{\left[2\pi nd(x)\right]/\left[\lambda\cos\theta_1\right]\right\}\bmod\{2\pi\} = a(x) \quad ;\left\{\left[2\pi nd(x)\right]/\left[\lambda\cos\theta_2\right]\right\}\bmod\{2\pi\} = b(x) \tag{1}$$

where λ is the wavelength, n is the refractive index of the sample, and d(x) is the true (unwrapped) profile that we wish to extract. Mod is the mathematical operation of modulo. The required angular change between images is less than one pixel in the camera.
The results of this setup are presented in Fig. 5. The first two images (Fig. 5. (a),(b)) are the phase reconstructions separated by a 1 degree specimen rotation. The lowest image (Fig. 5. (c)) is the reconstructed 3D profile computed from Eq. (1). This method allows imaging of phase only transparent objects and, in the case when the profile is known, allows refractive index estimation.
It is also possible to use speckle contrast instead of fringe contrast. Speckles are a random pattern created by a beam scattered from a rough surface. Each optical system has a unique speckle pattern that varies in the propagation direction (Goodman, 1984). This means that it is possible to generate for each axial position its own distinguishable random illumination pattern. Furthermore, the random patterns that are related to different planes have low correlation with each other. Hence, by recognizing the speckle pattern one may determine the axial location (Almoro & Hanson, 2008; Rastogi & Jacquot, 1987; Sjödahl, 1995). However, this approach is mainly used to measure distortion of an object and is usually combined with other methods. Furthermore, the speckle contrast decreases as the beam propagates along the axial direction. This allows phase retrieval through computation of speckle contrast (Irvine et. al., 2010). In both of these methods the speckle distributions are first studied. Then, the sample is placed in the setup and the depth is recovered from the reference speckle information.

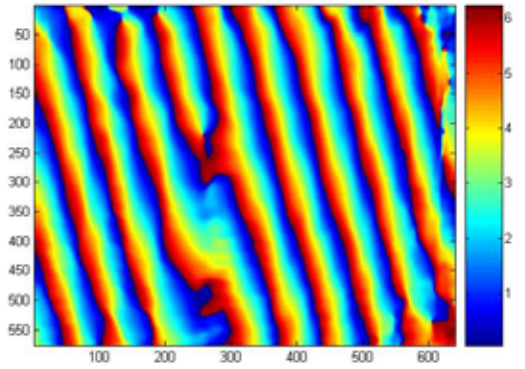

(a)

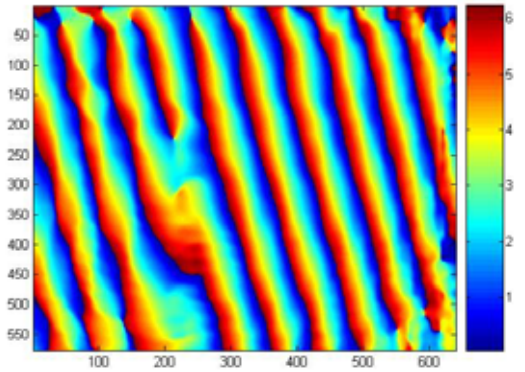

(b)

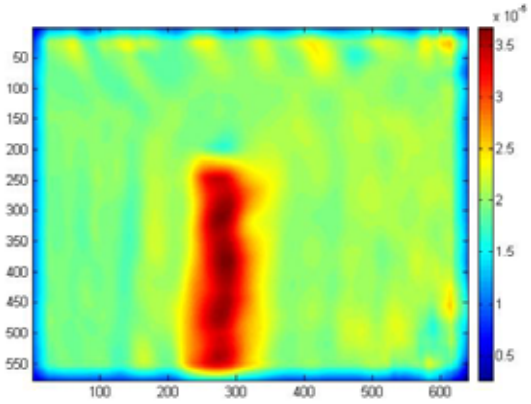

(c)

Fig. 5. Experimental reconstruction using rotation of specimen. (a),(b) Phase reconstruction for two projection angles that were separated by 1 degree. (c) Profile reconstruction. Each pixel represents a 6.7μm camera pixel. The alleviation thickness is in meters.

3. Numerical computations

The numerical computational methods allow phase reconstruction with or without an interferometer setup. However, they are needed for more than just phase retrieval. The digital computation of the wavefront propagation is also needed in any numerical algorithm or simulation of an electromagnetic wave. The different kinds of numerical reconstruction also offer a solution for difficulties in real space processing, such as spurious noise, fringes, optical system aberrations etc. There are numerous computational methods, including Kirchhoff–Helmholtz transform (Gabor, 1949), Fresnel-Kirchhoff (Cuche et. al., 1999), transforming Guigay equations (Guigay, 1977; Teague, 1983), solving transport of intensity equations (Gureyev & Nugent, 1997), convolution (Colomb et. al., 2006), angular spectrum (Mann et. al., 2005) etc. Each method corresponds to a different mathematical description of the optical space and has its advantages for a specific circumstance. Some descriptions are differential while others are integral.

One of the most common equations, which describe the propagation of an input wave u(x,0) through a free space distance z, is the Fresnel integral:

$$u(x,y,z) = \exp(i2\pi z/\lambda)\left[u(x,y,0) * \exp\left(i2\pi\left(x^2+y^2\right)/z\lambda\right)\right]/iz\lambda \tag{2}$$

where λ is the wavelength and * denotes the mathematical convolution operation. However, since numerical simulations are discrete, according to the Nyquist theorem this is correct only if $z>Z_c$, while Z_c is defined as:

$$Z_c = Ndx^2/\lambda \tag{3}$$

where N is the number of pixels and dx is the pixel size.

If one would like to represent the very near field, then there is need for a different approximation.

The angular spectrum calculation of the output field is

$$u(x,y,z) = \iint U(\xi,\mu)\exp\left(-i\pi\left(\xi^2+\mu^2\right)\lambda z\right)\exp\left(2\pi i(\xi x+\mu y)\right)d\xi d\mu \tag{4}$$

where U(ξ) is the Fourier transform of the input field, defined by

$$U(\xi,\mu) = \iint u(x,y,0)\exp\left(-2\pi i(\xi x+\mu y)\right)dxdy \tag{5}$$

The meaning of this representation is to compute the product between the Fourier transform of the input field and the Fourier transform of the Kernel $\exp(i\pi(x^2+y^2)/\lambda z)$. In this case the Nyquist theorem require $z<Z_c$ (Mendlovic et. al., 1997).

Mathematically, Eq. (3) and (4) are the same, since it is a known Fourier property that the convolution operation becomes a product in the Fourier domain. However, converting these equations from the continuous domain to the discrete one reveals a contradiction.

The transport of intensity equation indicates what is the input phase φ(x,y) that solves a known intensity I(x,y,z) variation in the propagation direction.

$$-\nabla\cdot(I(x,y,z)\nabla\varphi(x,y)) = 2\pi/\lambda\partial_z I(x,y,z) \tag{6}$$

where $\nabla=(\partial_x,\partial_y)$ is the gradient operator. By decomposing the problem to the Fourier harmonics, it is posible to convert the differential problem into a matrix formulae.

There are other advantages in choosing certain computational method. For example, the angular spectrum computation allows control of spurious noise components (Mann et. al., 2005).

4. Iterative phase retrieval

One famous iterative method is the Gerchberg-Saxton (GS) algorithm (Gerchberg & Saxton, 1972). This method is widely used to retrieve the input phase, from known amplitude distributions of the input and output fields of an optical setup. Later on this algorithm was used for beam shaping applications to compute the required phase element for producing a specific output intensity, given the input illumination. The idea is to choose an initial random phase estimation and compute a new estimation in each new iteration (Fig. 6).

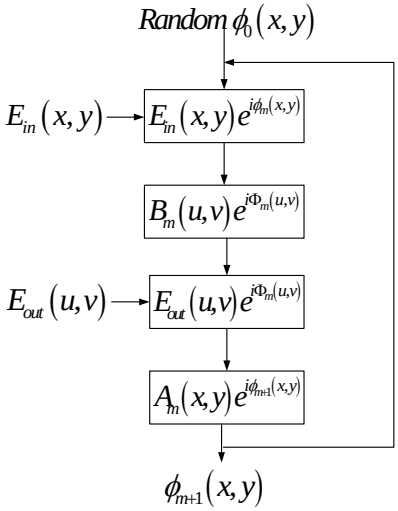

Fig. 6. A scheme of the GS algorithm.

In each iteration the contribution of the current phase estimation and the amplitude of the input illumination are computed, denoted by the input plane expression $E_{in}(x,y)\exp\{i\phi_m(x,y)\}$. Then, the resulting expression after passing through the optical domain is computed by transforming this input plane expression. This is denoted by the output plane expression $B_m(u,v)\exp\{i\Phi_{m+1}(u,v)\}$. In order to fulfill the apriori constrain for the output plane intensity, the magnitude of the output plane is replaced by $E_{out}(u,v)$. The output plane expression is now $E_{out}(u,v)\exp\{i\Phi_{m+1}(u,v)\}$. The new output plane expression, $E_{out}(u,v)\exp\{i\Phi_{m+1}(u,v)\}$, is then inverse transformed to the input plane, denoted by $A_m(x,y)\exp\{i\phi_{m+1}(x,y)\}$, and the apriori constrain for the input amplitude $E_{in}(x,y)$ is imposed on the input expression. The phase $\phi_{m+1}(x,y)$ is the new phase estimation. This process is repeated until convergence is obtained.

Note that it was proven that the GS algorithm indeed converges (Fienup, 1982), which means that the next phase estimation is at least as good as the previous one.

The original GS algorithm was used in a Fourier based optical setup. However, other optical transforms, such as the Fresnel and the fractional Fourier transform, were later on proven to be more efficient in terms of convergence rate (Zalevsky et. al., 1996).

Another iterative approach is the gradient search method (Fienup, 1993). This method has a better considered step size towards the desired phase, which allows faster convergence for multiple intensity constrains.
However, the problem with iterative methods is the phase ambiguity, resulting with converging to a local minima solution, which leads to an incorrect phase distribution. In order to overcome this problem, statistical methods (Nieto-Vesperinas et. al., 1988), stimulated annealing (Kirkpatrick et. al., 1983; Zhou et. al., 1999) and de-convolution methods (Seldin & Fienup, 1990) were proposed.

5. Iterative phase retrieval approach based upon multiple measurements

The concept of using multiple images was first suggested regarding the phase ambiguity in electron microscopy (Misell, 1973). Misell proposed that by taking several defocused images, one may later reconstruct a better phase using the iterative GS algorithm. This idea was implemented in later works as well (Redding et. al., 1998; Acton et. al., 2004; Brady & Fienup, 2006; Dean et. al., 2006). In order to capture such multiple plane images, one can change the axial position of the sample using a stepper motor (Barty et. al., 1998), change the position of the recording imaging device by using mechanical motion (Zhang et. al. 2003) or using defocusing implemented in a spatial light modulator in a motionless configuration (Camacho et. al., 2010).

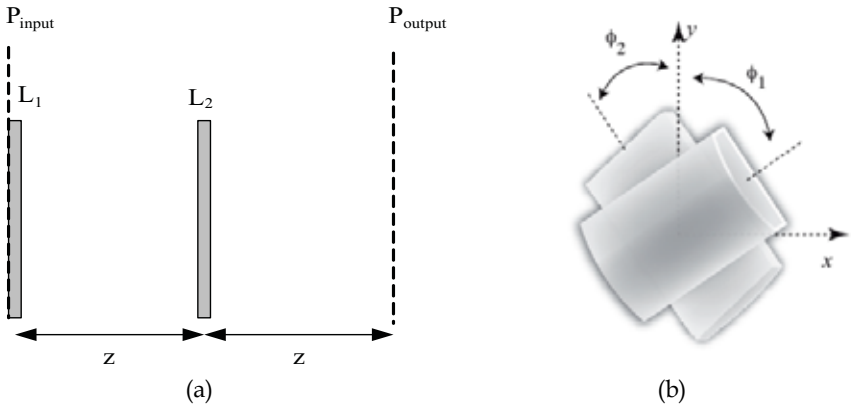

Fig. 7. (a) GT optical setup. Each generalized lens $L_{1,2}$ is an assembled set of two cylindrical lenses (b). The transformation is only reached by the proper rotation (with angles ϕ_1 and ϕ_2) of the lenses.

Recently the efficiency of the multiple constrains iterative method has been demonstrated using images obtained in the gyrator domains (Rodrigo et. al., 2010). The gyrator transform (GT) is a linear canonical integral transform, which produces the twisted rotation in position−spatial frequency planes of the phase space (Rodrigo et. al., 2007). Thus, the GT operation of a two dimensional function $f_i(r_i)$ (complex field amplitude) with a parameter α, known as the transformation angle, is given by

$$F^{\alpha}(r_o) = \frac{1}{2\lambda z|\sin\alpha|}\iint f_i(x_i, y_i)\exp\left(i2\pi\frac{(x_o y_o + x_i y_i)\cos\alpha - (x_i y_o + x_o y_i)}{2\lambda z\sin\alpha}\right)dx_i dy_i \quad (7)$$

where $\mathbf{r}_{i,o} = (x_{i,o}, y_{i,o})$ are the input and output coordinates, respectively, λz is a normalization parameter that for the case of the optical implementation of the GT correspond to the wavelength λ and to fixed axial interval between the lenses z. The gyrator projections $\left|F^{\alpha}(r_O)\right|^2$ can be measured using the optical setup displayed in Fig. 7 (a). The optical setup consists of two generalized lenses (Fig. 7 (a)). Each generalized lens is assembled from two cylindrical lenses (Fig. 7 (b)), properly rotated with angles ϕ_1 and ϕ_2 that fulfill the following relations with the transformation angle α:

$$\sin(2\varphi_1) = \cot(\alpha/2); \quad \sin(2\varphi_2) = (\sin\alpha)/2 \tag{8}$$

In order to improve phase retrieval in a gyrator base optical system it was proposed to use multiple rotation angles. As in the original GS algorithm, a random phase estimation is chosen, and in each iteration a new estimation is computed (Fig. 8). Note that this serial approach may also be used in different transformation domains than the gyrator e.g. in the Fresnel or the Fourier optical setups. Nevertheless the astigmatism of the GT allows to resolve some phase ambiguities (for example the direction of the rotation of the helicoidal phase) that is impossible to do using the isotropic transforms.

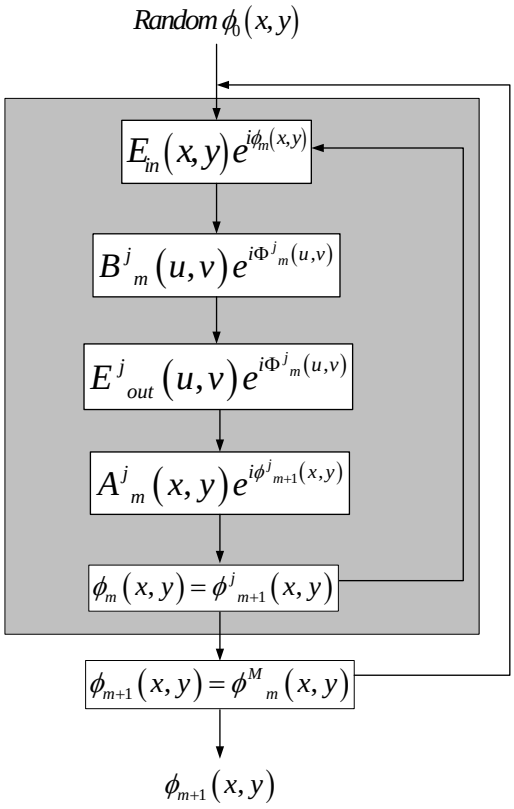

Fig. 8. Scheme of the iterative algorithm based upon multiple measurements.

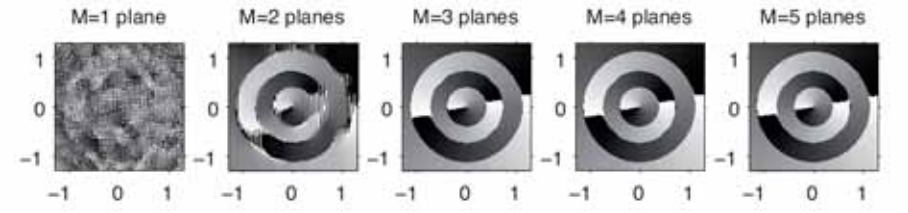

(a)

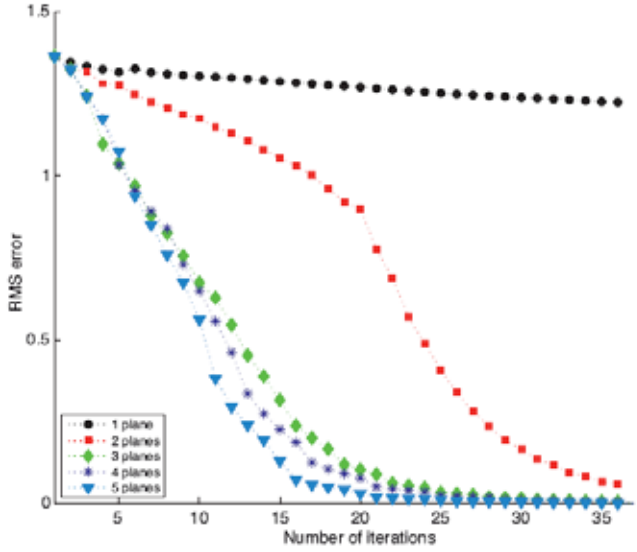

(b)

Fig. 9. Numerical results for the multi-stage phase retrieval algorithm using GT. M is the number of constraint images (measurements). (a) Retrieved phase distribution after 23 iterations for the case of $LG_{+3,1}$ mode. (b) The phase retrieval is calculated by using constraint images involving angles: α = 45°, 55°, 65°, 70° and 80°. The evolution of RMS error is also displayed as a function of the number of constraint images as well as the number of utilized iterations.

In order to estimate the phase retrieval capabilities of a multiple plane method in comparison to a single plane method, a quality measuring tool is need. A common image processing tool for this is the relative root mean square (RMS) error, also known as Abserr, which is given by

$$\mathrm{RMS} = \left(\sum \left| E_{in}\exp(i\phi) - E_{in}\exp(i\phi_{rt}) \right|^2\right)^{\frac{1}{2}} \times \left(\sum \left| E_{in}\exp(i\phi) \right|^2\right)^{-\frac{1}{2}} \tag{9}$$

where $\phi(x,y)$ is the phase to retrieve and $\phi_{rt}(x,y)$ is the estimated phase distribution at each iteration.

The reconstructed phase distribution for a different numbers of planes is shown in Fig. 9 (a). One may see that for a fixed number of iterations, the reconstructed phase improves as the

number of planes increases. The RMS error versus the number of iterations is shown in Fig. 9 (b). Adding planes decreases the convergence time. By defining successful retrieval as one having RMS error of less than 0.02, it was also demonstrated that the phase distribution is successfully retrieved (even in a noisy case) by using at least three constraint planes and after applying 36 iterations (Rodrigo et. al., 2010).
By working with the gyrator optical setup, instead of other optical domains, one may use images from different transform rotation angles (rather than using different axial positions requiring generation of axial movement) which makes the system more flexible and robust.

6. Conclusion

In this chapter we have presented an overview on the topic of the phase retrieval problem. We have presented some interesting perspectives in three different approaches: digital holography, iterative phase retrieval and multiple measurement methods.
First we have presented the interferometer as the optical setup needed for digital holography. We have discussed the advantages of in-phase setups as well. We have presented the problem of phase ambiguity in holography based methods. Our work of using partial coherence or specimen rotation was able to overcome this phase wrapping problem.
We have presented different computational methods needed in phase retrieval. The use of computational methods in digital holography is preferable over regular holography in terms of dealing with spurious noise, fringes, optical system aberrations etc.
Then we have discussed the abilities of various iterative methods having local minima solution problem. The idea of multiple measurements to create a multiple plane iterative method was presented as a possible solution. Out work implementing this approach in the gyrator domain was presented and was proven to allow phase retrieval with high accuracy and low complexity.
The phase retrieval methods, mentioned in this chapter, are commonly used in different three dimensional applications. Space telescopes, such as the James Webb space telescope (Acton et. al., 2004), use the multiple measurement iterative approach. Electron microscopy uses the multiple measurement method as well. Iterative phase retrieval algorithms are also used for planning diffractive optical elements (DOE) used as phase only filters for beam shaping (Zhou et. al., 1999). Digital holography microscopes (DHM) use different interferometer based setups (Charriere et. al., 2006).

7. References

Acton, D. S.; Atcheson, P. D.; Cermak, M.; Kingsbury, L. K.; Shi, F. and Redding, D. C. (2004). James Webb Space Telescope wavefront sensing and control algorithms, *Proceedings of SPIE 5487*, 887, Glasgow Scotland United Kingdom, June 2004, SPIE .

Almoro, P. F. and Hanson, S. G. (2008). Wavefront sensing using speckles with fringe compensation, *Opt. Exp.*, Vol. 16, No. 11, (May 2008) pp. 7608-7618.

Almoro, P. F.; Maallo, A. M. S. and Hanson, S. G. (2009) . Fast-convergent algorithm for speckle-based phase retrieval and a design for dynamic wavefront sensing, *Appl.* Opt., Vol. 48, No. 8, (Mar. 2009) pp. 1485-1493.

Barty, A.; Nugent, K. A.; Paganin,D. and Roberts, A. Quantitative optical phase microscopy, *Opt. Lett.*, Vol. 23, No. 11, (Jun. 1998) pp. 817-819.

Brady, G. R. and Fienup, J. R.(2006). Nonlinear optimization algorithm for retrieving the full complex pupil function, *Opt. Express*, Vol. 14, No. 2, (Jan. 2006) 474–486 .

Bruning, J. H.; Herriott, D. R.; Gallagher, J. E.; Rosenfeld, D. P.; White, A. D. and Brangaccio, D. J. (1974). Digital wavefront measuring interferometer for testing optical surfaces and lenses, *Appl. Opt.*, Vol. 13, No. 11, (Nov. 1974) pp. 2693–2703.

Camacho, L.; Micó, V.; Zalevsky, Z. and García, J. Quantitative phase microscopy using defocusing by means of a spatial light modulator, *Opt. Express*, Vol. 18, No. 7 (Mar. 2010) pp. 6755-6766.

Cederquist, J N; Fienup, J R; Marron, J C; Paxman, R G (1988). Phase retrieval from experimental far-field speckle data, *Opt. Lett.*, Vol. 13, No. 8, (Aug. 1988) pp.619-621

Charriere, F.; Marian, A.; Montfort, F.; Kuehn, J. and Colomb, T. (2006). Cell refractive index tomography by digital holographic microscopy, *Opt. Lett.*, Vol. 31, No. 2, (Jan. 2006) pp. 178-180.

Choi, W.; Fang-Yen, C; Badizadegan, K.; Dasari, R. R. And Feld, M. S. (2008). Extended depth of focus in tomographic phase microscopy using a propagation algorithm, *Opt. Lett.*, Vol. 33, No. 2, (Jan. 2008) pp. 171-173.

Colomb, T.; Montfort, F.; Kuhn,J; Aspert, N.; Cuche, E.; Marian, A.; Charrier, F.; Bourquin, S.; Marquet, P. and Depeursinge, C. (2006). Numerical parametric lens for shifting, magnification, and complete aberration compensation in digital holographic microscopy, *JOSA A.*, Vol. 23, No. 12, (Dec. 2006) pp. 3177-3190.

Cuche, E.; Bevilacqua, F. and Depeursinge, C. (1999). Digital holography for quantitative phase-contrast imaging, *Opt. Lett.*, Vol. 24, No. 5, (Mar. 1999) pp. 291–293.

Dean, B. H.; Aronstein, D. L.; Smith, J. S.; R. Shiri, and Acton, D. S. (2006). Phase retrieval algorithm for JWST Flight and Testbed Telescope, *Proceedings of SPIE 6265*, 626511, Orlando FL USA, May 2006, SPIE.

Fienup, J. R. (1982). Phase retrieval algorithms: a comparison, *Appl. Opt.*, Vol. 21, No. 15, (Aug. 1982) pp. 2758-2769.

Fienup, J. R. (1993). Phase-retrieval algorithms for a complicated optical system, *Appl. Opt.*, Vol. 32, No. 10, (Apr. 1993) pp. 1737–1746 .

Gabor, D. (1948). A new microscopic principle, *Nature*, Vol. 161, No. 4098, (May 1948) pp. 777–778.

Gabor, D. (1949). Microscopy by reconstructed wavefronts, *Proc. R. Soc. London Ser. A*, Vol. 197, No. 1051, (Jul. 1949) pp. 454–487.

Gerchberg ,R. W. and Saxton, W. O. (1972). A practical algorithm for the determination of phase from image and diffraction plane pictures, *Optik*, Vol. 35, No. 2 237–246.

Goodman, J. W. (2000). *Statistical optics*, Wiley Interscince, ISBN 0471399167, New York.

Guigay, J. P. (1977). Fourier-transform analysis of Fresnel diffraction patterns and in-line holograms, *Optik*, Vol. 49, pp. 121–125.

Gureyev, T. E. and Nugent, K. A. (1997). Rapid quantitative phase imaging using the transport of intensity equation, *Opt. Commun.*, Vol. 133, No.1, (Jan. 1997) pp.339 – 346.

Irvine, S. C.; Paganin, D. M.; Jamison, R. A.; Dubsky, S. and Fouras, A. (2010). Vector tomographic X-ray phase contrast velocimetry utilizing dynamic blood speckle, *Opt. Exp.*, Vol. 18, No. 3, (Jan. 2010) pp. 2368-2379.

Karo, D. P. and Schneiderman, A. M.(1977). Transfer functions, correlation scales, and phase retrieval in speckle interferometry, *JOSA*, Vol. 67, No, 11, (Nov. 1977) pp. 1583-1587.

Kirkpatrick, S.; Gelatt, C. D. and Vecchi, M. P. (1983). Optimization by simulated annealing, *Scienc,e* Vol. 220, No. 4598 , (May 1983) pp. 671–680.

Leith, E. N. and Upatnieks, J. (1962). Reconstructed wavefronts and communication theory, *JOSA*, Vol. 52, No. 10, (Oct. 1962) pp. 1123– 1128.

Leith, E. N. and Upatnieks, J. (1963). Wavefront reconstruction with continuous-tone objects, *JOSA*, Vol. 53, No. 12, (Dec. 1963) pp. 1377–1381.

Leith, E. N. and Upatnieks,J. (1964). Wavefront reconstruction with diffused illumination and three-dimensional objects, *JOSA*, Vol. 54, No. 11, (Nov. 1964) 1295–1301.

Mann, C.; Yu, L.; Lo, C. M. and Kim,M. (2005). High-resolution quantitative phase-contrast microscopy by digital holography, *Opt. Express*, Vol. 13, No. 22, (Oct. 2005) pp. 8693–8698.

Mendlovic, D.; Zalevsky, Z. and Konforti, N. (1997). Computation considerations and fast algorithms for calculating the diffraction integral, *J. Mod. Opt.*, Vol. 44, No. 2, (Feb. 1997) pp. 407-414.

Misell, D. L. (1973). A method for the solution of the phase problem in electron microscopy, *J. Phys. D: App. Phy.*, Vol. 6, No. 1,(Jan. 1973) pp. L6–L9.

Nieto-Vesperinas, M.; Navarro, R. and Fuentes, F. J. (1088). Performance of a simulated-annealing algorithm for phase retrieval, *JOSA A*, Vol. 5, No. 1, (Jan. 1988) pp. 30–38.

Rastogi, P. K and Jacquot, P. (1987). Measurement of difference deformation using speckle interferometry, *Opt. Lett.*, Vol. 12, No. 8, (Aug. 1987) pp. 596-598.

Redding, D. C.; Basinger, S.; Lowman, A.; Kissil, A.; Bely, P.; Burg, R.; Lyon, R.; Mosier, G.; Femiano,M.; Wilson, M.; Schunk, R. G.; Craig, L.; Jacobson, D.; Rakoczy, J. and Hadaway ,J. (1998). Wavefront Sensing and Control for a Next- Generation Space Telescope, *Proceedings of SPIE 3356*, 758,Liege Belguim, Jun. 1998.

Rodrigo, J. A.; Alieva, T. and Calvo, M. L. (2007). Experimental implementation of the gyrator transform, *JOSA A* , Vol. 24, No. 10,(Oct. 2007) pp. 3135–3139.

Rodrigo, J. A.; Duadi, H.; Alieva, T. and Zalevsky, Z. (2010). Multi-stage phase retrieval algorithm based upon the gyrator transform, *Opt. Exp.*, Vol. 18, No. 2, (Jan. 2010) pp. 1510–1520 .

Rosen, J. and Yariv, A. (1996). General theorem of spatial coherence: application to three-dimensional imaging, *JOSA A*, Vol. 13, No. 10, (Oct. 1996) 2091–2095.

Seldin, J. H. and Fienup, J. R. (1990). Iterative blind deconvolution algorithm applied to phase retrieval, *JOSA A*, Vol. 7, No. 3, (Mar. 1990) pp. 428–433 .

Sjödahl, M (1995). Calculation of speckle displacement, decorrelation, and object-point location in imaging systems, *Appl. Opt.* Vol. 34, No. 34,(Dec. 1995) pp. 7998-8010.

Teague, M. R. (1983). Deterministic phase retrieval: a Green's function solution, *JOSA*, Vol. 73, No. 11, (Nov. 1983) pp. 1434–1441.

Xu, W.; Jericho, M. H.; Meinertzhagen, I. A. and Kreuzer, H. J. (2002). Digital in-line holography of microspheres, *Appl. Opt.*,Vol. 41, No. 25, (Sep. 2002) 5367–5375 .

Yamaguchi, I. and Zhang, T. (1997). Phase-shifting digital holography, *Opt. Lett.*, Vol. 22, No. 16, (Aug. 1997) pp. 1268-1270.

Zalevsky, Z.; Mendlovic, D. and Dorsch, R. G. (1996). Gerchberg-Saxton algorithm applied in the fractional Fourier or the Fresnel domain, *Opt. Lett.*, Vol. 21, No. 12, (Jun. 1996) pp. 842-844.

Zalevsky, Z.; Margalit, O.; Vexberg, E.; Pearl, R. and Garcia, J. (2008). Suppression of phase ambiguity in digital holography by using partial coherence or specimen rotation, *App. Opt.*, Vol. 47, No. 19, (Apr. 2008) pp. D154-D163.

Zhang, Y.; Pedrini, G.; Osten, W. and Tiziani, H. Whole optical wave field reconstruction from double or multi in-line holograms by phase retrieval algorithm, *Opt. Express*, Vol. 11, No. 24 (Dec. 2003) pp. 3234–3241.

Zhou, G.; Chen, Y.; Wang, Z. and Song, H. (1999). Genetic Local Search Algorithm for Optimization Design of Diffractive Optical Elements, *Appl. Opt.*, Vol. 38, No. 20, (Jul. 1999) pp. 4281-4290.